Supporting Information

Derrien et al. 10.1073/pnas.1209487109

SI Experimental Procedures

Plant Lines and Growth Conditions. *Arabidopsis thaliana* mutants *ago1-11* (1), *ago1-25*, *ago1-27* (2), *hen1-1* (3), *hyl1-2*, *dcl1-9* (4), *hst* (5), *amsh3-1* (6), and the G548 line (7) were described previously. XVE-P0^{BW}-myc line was generated by agrotransformation of *A. thaliana* Col-0 plant with pXVE-P0^{BW}-myc construct. GFP-AGO1 lines were generated by complementation of *ago1-27* and *ago1-11* mutants with the pAGO1:GFP-AGO1 construct. The pXVE-P0^{BW} (L21) transgenic line (8) was crossed with the GFP-AGO1 line to generate the P0/GFP-AGO1 lines.

For in vitro culture, seeds were surface sterilized using ethanol, plated on germination medium [MS salts (Duchefa), 1% sucrose, 0.8% agar (pH 5.6)], stored 2–3 d at 4 °C in the dark, and then transferred to a plant growth chamber under a 16 h light/8 h dark) photoperiod (22 °C/20 °C).

Transient Expression Assays in *N. benthamiana*. Binary constructs were transformed in *Agrobacterium tumefaciens* GV3101 and then transformed in *N. benthamiana* for transient expression assays. *Agrobacterium* cells were grown overnight at 28 °C in 5–10 mL LB medium supplemented with antibiotics, resuspended in 10 mM $MgCl_2$ 200 mM acetosyringone at an OD of 0.5 per construct, and incubated for 2–4 h at room temperature before being pressure infiltrated into leaves of 4-wk-old plants. Plants were maintained in growth chambers under a 16 h light/8 h dark photoperiod with a constant temperature of 22 °C. Observations under the microscope were performed 48 h after agrotransformation. When treatments were applied (E64d 20 μM), drugs were mixed in 10 mM $MgCl_2$ and pressure infiltrated into leaves 12–16 h before observation.

RNA Analyses by Northern Blotting and qRT-PCR. RNA extraction was performed on *Arabidopsis* seedlings using TRI Reagent (Sigma) according to the manufacturer's instructions. RNA gel blot analyses of low- and high-molecular-weight RNA were performed with 20 and 10 μg of total RNA, respectively. mRNAs were separated on 1,1 M formaldehyde 1% agarose gel, and blotted onto Hybond-N (Amersham) membrane. Low-molecular-weight RNAs were separated on acrylamide gel using the procedure described in Hamilton and Baulcombe, 1999 (9) and electroblotted on Hybond-NX (Amersham) membrane. For mRNA, methylene blue staining of total RNA was performed directly after transfer to confirm equal loading. Radiolabeled probe for detection of the AGO1 mRNA was made by random priming reactions in presence of [α-^{32}P]dCTP (Amersham). The template used was a PCR product amplified from AGO1 cDNA with primers described in Vaucheret et al., 2006 (10). DNA oligonucleotides complementary to miR168 and U6 were end labeled with [γ-^{32}P]ATP using T4 PNK (New England Biolabs). Hybridization was performed overnight in perfectHyb Plus (Sigma) at 65 °C for mRNA probes and 42 °C for low-molecular-weight RNA probes.

For quantitative RT-PCR (qPCR), total RNA was extracted from 2-wk-old seedlings grown on MS agar plates, the TRI Reagent method (see above). In all assays, 5 μg of total RNA treated with DNase RQ1 was reverse transcribed with AB (Applied Biosystems) high-capacity cDNA reverse transcription kit (random hexamer). PCR was performed using AGO1-specific primers (Table S1) in a total volume of 10 μL SYBR Green Master mix (Roche) on a Lightcycler LC480 apparatus (Roche) according to the manufacturer's instructions. The mean value of three replicates was normalized using the *GAPDH* (AT1G16300) gene as internal control.

Constructs. ***pXVE-P0^{BW}-myc line.*** A BWYV P0 clone (8) was produced with an in-frame triple Myc-tag (GEQKLISEEDLN) at the C terminus of the P0 protein and introduced into the XhoI-SpeI sites of pER8 (11). The resulting pXVE-P0myc plasmid was mobilized into *Agrobacterium tumefaciens* strain GV3101 and further used to transform *A. thaliana* (ecotype Col-0) according to Bechtold and Pelletier, 1998 (12). Segregation of T2 seeds was analyzed and single T-DNA insertion lines were tested for P0 expression and AGO1 degradation.

pAGO1:GFP-AGOA1 line. The GFP-AGO1 construct was generated as described in Baumberger and Baulcombe, 2005 (13) except that the 5′ primer used for amplification and cloning of *AGO1* coding sequence has been modified to remove Flag-tag to generate the pAGO1:AGO1 vector. Then GFP was PCR amplified from pK7FWG2 (Ghent plasmids collection, http://bccm.belspo.be/index.php) and cloned into pAGO1:AGO1 vector at the 5′ end of AGO1 coding sequence using XhoI restriction site to create pAGO1:GFP-AGO1 plasmid. This vector was mobilized into *A. tumefaciens* strain GV3101 together with pSoup plasmid and further used to transform *Arabidopsis ago1-27* or *ago1-11* mutants. Complementation of *ago1-11* and *ago1-27* was checked in T2 and T3 plants as well as segregation of BASTA resistance in T2 seeds to select single T-DNA insertion lines.

p35S:RFP-ATG8a construct. ATG8a coding sequences were cloned by recombination into the destination vectors pK7RWG2 (Ghent plasmids collection, http://bccm.belspo.be/index.php) to obtain RFP–ATG8a fusion. The plasmid was then mobilized into *A. tumefaciens* strain GV3101 and used for transient expression assays in *N. benthamiana*.

p35S:GFP-AGO1 construct. *AGO1* coding sequences were cloned by recombination into the destination vectors pK7FWG2 (Ghent plasmids collection, http://bccm.belspo.be/index.php) to obtain GFP–AGO1 fusion. The plasmid was then mobilized into *A. tumefaciens* strain GV3101 and used for transient expression assays in *N. benthamiana*.

p35S:P0^{BW} has been already described in Baumberger et al., 2007 (14)

List of primers for cloning and qRT-PCR is indicated in Table S1.

1. Kidner CA, Martienssen RA (2004) Spatially restricted microRNA directs leaf polarity through ARGONAUTE1. *Nature* 428:81–84.
2. Morel J-B, et al. (2002) Fertile hypomorphic ARGONAUTE (ago1) mutants impaired in post-transcriptional gene silencing and virus resistance. *Plant Cell* 14:629–639.
3. Chen X, Liu J, Cheng Y, Jia D (2002) HEN1 functions pleiotropically in Arabidopsis development and acts in C function in the flower. *Development* 129:1085–1094.
4. Song L, Han M-H, Lesicka J, Fedoroff N (2007) Arabidopsis primary microRNA processing proteins HYL1 and DCL1 define a nuclear body distinct from the Cajal body. *Proc Natl Acad Sci USA* 104:5437–5442.
5. Park M-Y, Wu G, Gonzalez-Sulser A, Vaucheret H, Poethig RS (2005) Nuclear processing and export of microRNAs in Arabidopsis. *Proc Natl Acad Sci USA* 102:3691–3696.
6. Isono E, et al. (2010) The deubiquitinating enzyme AMSH3 is required for intracellular trafficking and vacuole biogenesis in Arabidopsis thaliana. *Plant Cell* 22:1826–1837.
7. Deprost D, et al. (2007) The Arabidopsis TOR kinase links plant growth, yield, stress resistance and mRNA translation. *EMBO Rep* 8:864–870.
8. Bortolamiol D, Pazhouhandeh M, Marrocco K, Genschik P, Ziegler-Graff V (2007) The Polerovirus F box protein P0 targets ARGONAUTE1 to suppress RNA silencing. *Curr Biol* 17:1615–1621.
9. Hamilton AJ, Baulcombe DC (1999) A species of small antisense RNA in posttranscriptional gene silencing in plants. *Science* 286:950–952.
10. Vaucheret H, Mallory AC, Bartel DP (2006) AGO1 homeostasis entails coexpression of MIR168 and AGO1 and preferential stabilization of miR168 by AGO1. *Mol Cell* 22:129–136.

11. Zuo J, Niu QW, Chua NH (2000) Technical advance: An estrogen receptor-based transactivator XVE mediates highly inducible gene expression in transgenic plants. *Plant J* 24:265–273.
12. Bechtold N, Pelletier G (1998) In planta Agrobacterium-mediated transformation of adult Arabidopsis thaliana plants by vacuum infiltration. *Methods Mol Biol* 82: 259–266.
13. Baumberger N, Baulcombe DC (2005) Arabidopsis ARGONAUTE1 is an RNA Slicer that selectively recruits microRNAs and short interfering RNAs. *Proc Natl Acad Sci USA* 102: 11928–11933.
14. Baumberger N, Tsai C-H, Lie M, Havecker E, Baulcombe DC (2007) The Polerovirus silencing suppressor P0 targets ARGONAUTE proteins for degradation. *Curr Biol* 17: 1609–1614.

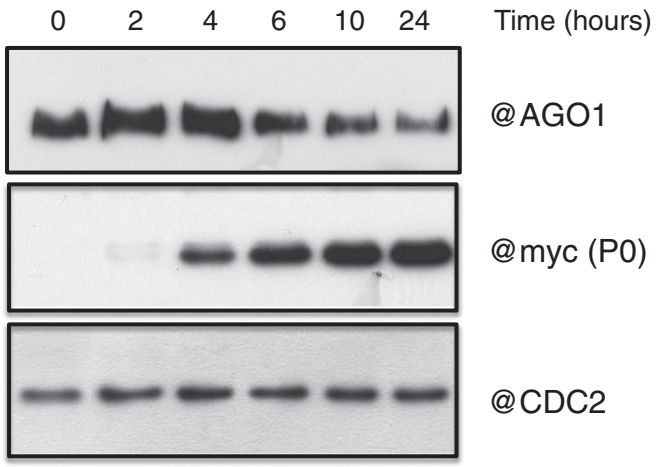

Fig. S1. Induction of P0 expression leads to AGO1 decay. AGO1 degradation kinetics were performed on 7-d-old XVE-P0^{BW}-myc seedlings transferred to liquid MS medium supplemented with β-estradiol (5 μM) for P0-myc induction. The accumulation level of AGO1, P0-myc, and CDC2 (loading control) was assayed by Western blot.

Fig. S2. The pAGO1:GFP-AGO1 construct complements *ago1-11* mutant allele. (*Upper*) Complementation of *ago1-11* phenotype by the pAGO1:GFP-AGO1 construct and (*Lower*) the GFP signal in root tip of a complemented plant. Close-up images of root tip cells show a cytoplasmic localization of GFP-AGO1. GFP-AGO1 localization is not homogenous and in some cells is more concentrated around the nuclear envelop.

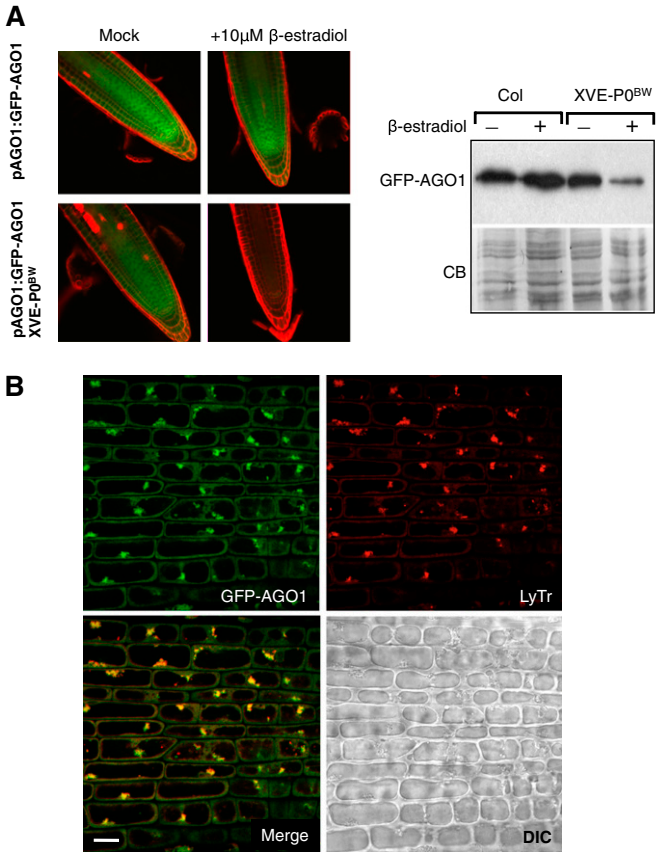

Fig. S3. GFP-AGO1 is degraded upon induction of P0, but is stabilized by E64d in acidic vesicular-shaped structures. (*A*) P0-mediated degradation of GFP-AGO1 assayed by confocal microscopy (*Left*) or by Western blot (*Right*). Seedlings were germinated on vertical MS plates with 10 μM β-estradiol and observed after 3 d. GFP-AGO1 was detected with an anti-GFP antibody and Coomassie blue staining is shown as loading control. (*B*) When P0 induction is combined with E64d (20 μM) treatment, GFP-AGO1 is stabilized and accumulates in vesicular-shaped structures that colocalize with acidic vesicles labeled with LysoTracker Red DND-99. Images were taken from 7-d-old seedlings after 16–18 h of P0 induction in presence of E64d. (Scale bars: 10 μm.)

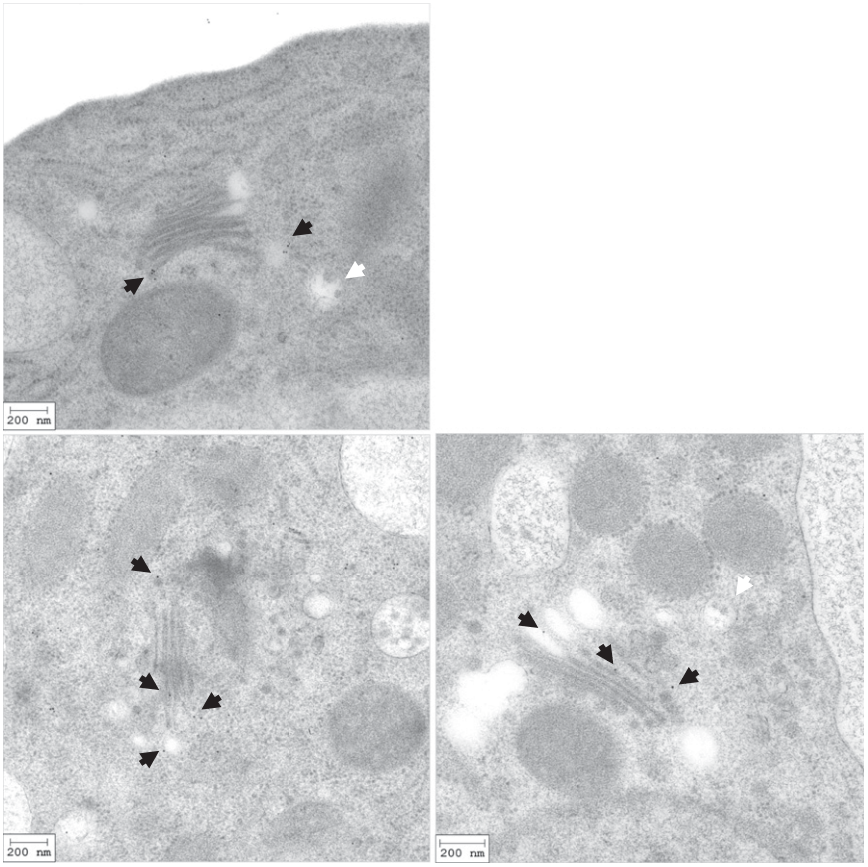

Fig. S4. AGO1 is enriched at proximity of the Golgi apparatus. Immunogold labeling of GFP-AGO1 was performed on 7-d-old seedlings after 16–18 h of P0 induction and additional treatment with the protease inhibitor E64d. It revealed that AGO1 is enriched at proximity of the Golgi apparatus (black arrows), but was not detected in MVBs (white arrows). (Scale bar: 200 nm.)

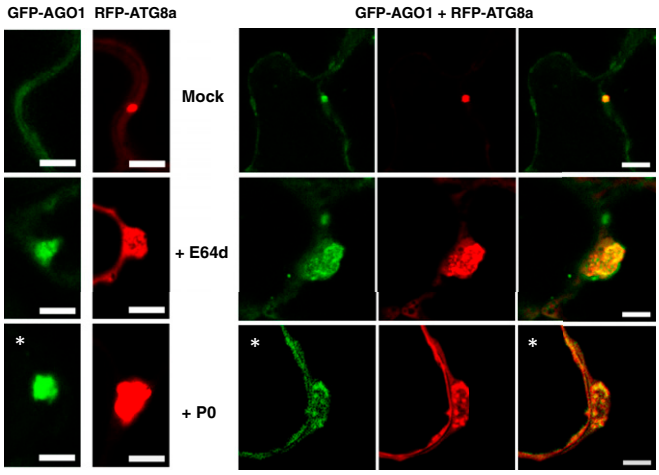

Fig. S5. AGO1 colocalizes with ATG8a in plant cells. (*Left*) GFP-AGO1 and RFP-ATG8a localization when individually transiently expressed into *N. benthamiana* leaves. As has been observed in *A. thaliana*, E64d triggers stabilization of GFP-AGO1 inside vesicular-shaped structures and P0 coexpression also induces the formation of such similar structures. In the case of RFP-ATG8a, small RFP-ATG8a-labeled vesicles were observed and their size was increased either by E64d treatment or by P0 coexpression. (*Right*) Coexpression of GFP-AGO1 and RFP-ATG8a in *N. benthamiana* leaves. E64d treatment and P0 coexpression revealed that both proteins colocalized inside vesicles as shown on the merged pictures (*Right*). The asterisk (*) indicates that the brightness of these pictures has been increased because of lower levels of GFP-AGO1 protein due to P0-dependant degradation.

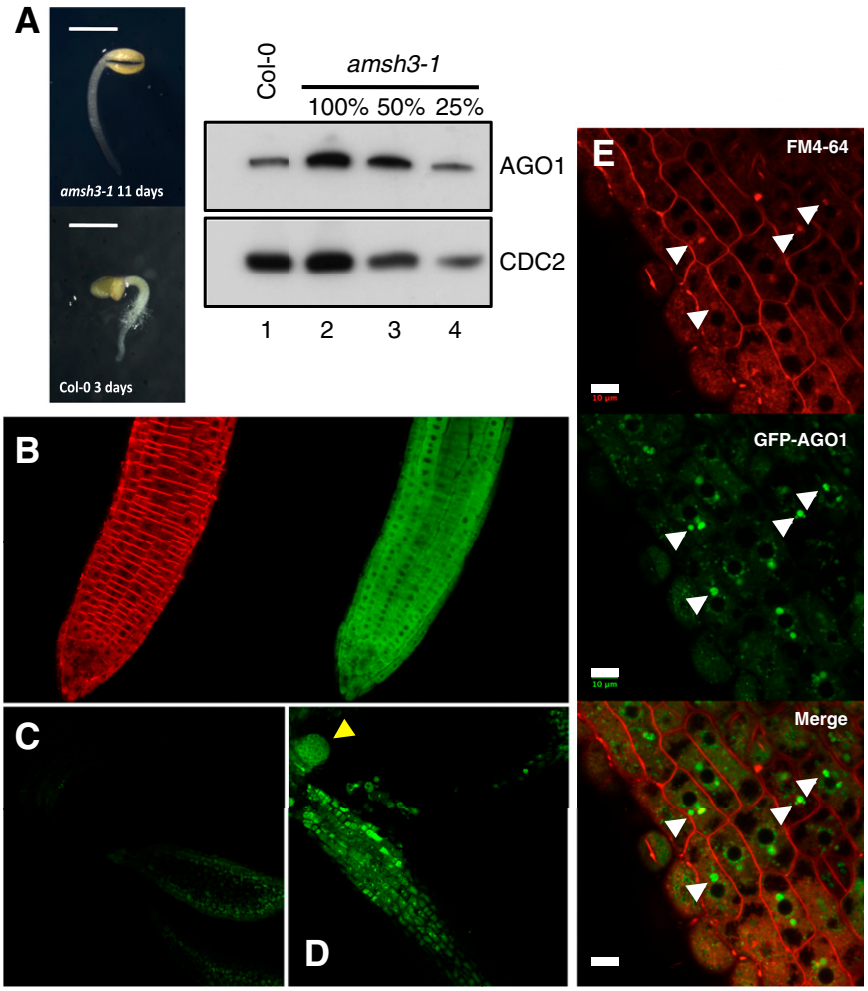

Fig. S6. AGO1 degradation is affected in homozygous *amsh3-1* mutant. (*A*) Relative AGO1 protein content in homozygous *amsh3-1* mutant seedlings compared with wild-type Col-0. (*Left*) The seedlings that were used for protein extraction; to use plant material at a similar developmental stage, homozygous *amsh3-1* seedlings were collected 11 d after germination and Col-0 seedlings 3 d after germination. Protein extracts were analyzed by Western blot using antibodies raised against AGO1 and CDC2 (as loading control); lanes 1 and 2 (20 μg), lane 3 (10 μg), and lane 4 (5 μg) of total proteins, respectively. Confocal microscopy images show a high level of GFP-AGO1 in the root tip (*B*) in an *amsh3-1* genetic background. Moreover, the GFP-AGO1 protein was also detected in aerial parts of *amsh3-1* mutant seedlings (*D*), and the GFP-AGO1 signal in wild-type cotyledons is very faint (*C*). The arrow indicates the apical meristem. In *amsh3-1* cotyledon cells, GFP-AGO1 is mainly observed in globular-shaped structures that are also marked by the FM4-64 membrane dye (*E*).

Table S1. List of primers for cloning and qRT-PCR

VRF AGO1 87 Fw	F	CGGTGGACAGAAGTGGGAAT	qPCR
VRF AGO1 87 Rv	R	GGTCGAGAAGTGCCCTGAAT	qPCR
GAPDH	F	TTGGTGACAACAGGTCAAGCA	qPCR
GAPDH	R	AAACTTGTCGCTCAATGCAATC	qPCR
5′-Xho-AGO1_CDS	F	GTAC**CTCGAG***ATG*GTGAGAAAGAGAAGAACGGA	Cloning
5′-Xho-GFP	F	catc**CTCGAG***ATG*GTGAGCAAGGGCGAGGAG	Cloning
3′-Xho-GFP	R	ccat**CTCGAG**CTTGTACAGCTCGTCCATGCC	Cloning
attB1-ATG8a	F	GGGGACAAGTTTGTACAAAAAAGCAGGCTTAATGATCTTTGCTTGCTTG	Cloning
attB2ATG8a	R	GGGGACCACTTTGTACAAGAAAGCTGGGTTAGCAACGGTAAGAGATCC	Cloning
attB1AGO1	F	GGGGACAAGTTTGTACAAAAAAGCAGGCTCAATGGTGAGAAAGAGAAG	Cloning
attB2AGO1	R	GGGGACCACTTTGTACAAGAAAGCTGGGTCTCAGCAGTAGAACATGACAC	Cloning

Bold underlined characters indicate the position of restriction sites; F, forward primer; R, reverse primer.